

Exact time autocorrelation function of the N -spin classical Heisenberg equivalent neighbor model

Richard A. Klemm* and Marco Ameduri†
*Max-Planck-Institut für Physik komplexer Systeme,
 Nöthnitzer Straße 38, D-01187 Dresden, Germany*
 (Dated: October 25, 2018)

We reduce the autocorrelation function $\mathcal{C}_{11}(t)$ of the equivalent neighbor model of N classical spins exhibiting Heisenberg dynamics and exchange coupling J to quadrature. As the temperature $T \rightarrow \infty$, $\mathcal{C}_{11}(t) \propto t^{-N}$ for $Jt \gg 1$. At low T , the antiferromagnetic $\mathcal{C}_{11}(t)$ is a simple function of $(JT)^{1/2}t$, exhibiting strong frustration, but the ferromagnetic $\mathcal{C}_{11}(t)$ oscillates in a single mode the frequency of which approaches NJ as $T \rightarrow 0$. We conjecture that as $T \rightarrow \infty$, the near-neighbor correlation functions of N -spin classical Heisenberg rings are simply obtained from these results.

PACS numbers: 05.20.-y, 75.10.Hk, 75.75.+a, 05.45.-a

Recently, there has been a considerable interest in the physics of magnetic molecules. [1] These consist of small clusters of magnetic ions imbedded within a non-magnetic ligand group, which may crystalize into large, well-ordered single crystals of sufficient quality for neutron scattering studies. Each type of magnetic molecule is characterized not only by the number N of spins in the molecule, but also by the spatial configuration of the spins. Many examples of rings exist, [2, 3] but there are also examples of denser clusters. [1, 4] Usually, the spins interact mainly via the Heisenberg exchange interaction. Although interest in the dynamics of Heisenberg spin rings has been strong for many years, most of the work involved numerical simulation of the two-spin correlation functions. Recently, however, exact results for the Heisenberg dimer, isosceles and equilateral triangle, and four-spin ring were presented, [5, 6, 7] but larger rings can not be solved using this technique.

The equivalent neighbor model is the simplest model for the dynamics of a nanomagnet, first proposed by Kittel and Shore.[8] In this model, every spin interacts equally with all of the others. Although the Heisenberg dynamics of the $N \rightarrow \infty$ limit at infinite temperature T were obtained previously, [9] they have not yet been solved for $5 \leq N < \infty$. Although this model is oversimplified for direct comparison with experiment when $N \geq 5$, its exact solution could serve as a benchmark for future theoretical and experimental studies.

In this letter, we present an exact single integral representation of the autocorrelation function $\mathcal{C}_{11}(t)$ for the equivalent neighbor model with arbitrary N and T , both for ferromagnetic (FM) and antiferromagnetic (AFM) exchange couplings. As $T \rightarrow \infty$, an accurate asymptotic $1/N$ expansion is found. As $T \rightarrow 0$, the AFM $\mathcal{C}_{11}(t)$ reduces exactly to a simple function of $(JT)^{1/2}t$ for arbitrary N . For the FM case at low T , $\mathcal{C}_{11}(t)$ oscillates in a single mode with a frequency that approaches NJ as $T \rightarrow 0$, and a shape that fits a scaling relation. From additional studies of three- and four-spin rings with various amounts of bridging spins that interact only with the ring

spins, we conjecture that the long-time $T \rightarrow \infty$ asymptotic limit values of the near-neighbor correlation functions for equivalent neighbor coupling and near-neighbor coupling in classical Heisenberg N -spin rings are identical.

The Hamiltonian of the N -spin classical Heisenberg equivalent neighbor model is $H = -Js^2/2$, where the total spin $\mathbf{s} = \sum_{i=1}^N \mathbf{s}_i(t)$ is a constant. The dynamics are given by $d\mathbf{s}_i(t)/dt = J\mathbf{s}_i \times \mathbf{s}$, where $s_i = |\mathbf{s}_i| = 1$. $\mathbf{s}_i(t)$ may be written as $\mathbf{s}_1(t) = s_{1,\parallel} \hat{\mathbf{s}} + s_{1,\perp} [\hat{\mathbf{x}} \cos(st^*) - \hat{\mathbf{y}} \sin(st^*)]$, where $t^* = Jt$, $\hat{\mathbf{s}} = \hat{\mathbf{x}} \times \hat{\mathbf{y}}$, $s_{1,\parallel}(s, x) = (s^2 + 1 - x^2)/(2s)$, $x = |\mathbf{s} - \mathbf{s}_1|$, and $s_{1,\parallel}^2 + s_{1,\perp}^2 = 1$. Letting $\alpha = J/(2k_B T)$, where k_B is Boltzmann's constant, the autocorrelation function $\mathcal{C}_{11}(t) = \langle \mathbf{s}_1(t) \cdot \mathbf{s}_1(0) \rangle$ may be written

$$\mathcal{C}_{11}(t) = \frac{1}{Z_N} \int_0^{N-1} \mathcal{D}_{N-1}(x) dx \int_{|x-1|}^{x+1} s e^{\alpha s^2} ds \times [s_{1,\parallel}^2(s, x) + \cos(st^*) s_{1,\perp}^2(s, x)], \quad (1)$$

where the partition function $Z_N = \int_0^N 2s \mathcal{D}_N(s) e^{\alpha s^2} ds$ and $\mathcal{D}_N(s)$ is the N -spin density of states. $\mathcal{D}_N(x)$ is piecewise continuous,

$$\mathcal{D}_N(x) = \Theta(x) \sum_{p=0}^{E[(N-1)/2]} \Theta(N - 2p - x) \times \Theta(x - N + 2p + 2) d_{N-2p}(x), \quad (2)$$

$$d_{N-2p}(x) = \sum_{k=0}^p \frac{(-1)^k (N - 2k - x)^{N-2}}{2^{N-1} (N-2)!} \binom{N}{k}, \quad (3)$$

where $\Theta(x)$ is the Heaviside step function, $\binom{n}{m}$ are binomial distribution coefficients, and $E(x)$ is the largest integer in x . The near-neighbor correlation function $\mathcal{C}_{12}(t) = \langle \mathbf{s}_1(t) \cdot \mathbf{s}_2(0) \rangle$ is simply obtained from $\mathcal{C}_{11}(t)$ and the sum rule $\langle s^2 \rangle / N = 1 = \mathcal{C}_{11}(t) + (N-1)\mathcal{C}_{12}(t)$.

It is useful to write $\delta\mathcal{C}_{11}(t) = \mathcal{C}_{11}(t) - \lim_{t \rightarrow \infty} \mathcal{C}_{11}(t)$. Since $\mathcal{C}_{11}(0) = 1$, it suffices to obtain $\delta\mathcal{C}_{11}(t)$ for all t . Af-

ter some algebra, we have reduced $\delta\mathcal{C}_{11}(t)$ to quadrature,

$$\delta\mathcal{C}_{11}(t) = \sum_{p=0}^{E[(N-1)/2]} \int_{N-2p-2}^{N-2p} ds \cos(st^*) f_{N-2p}(s), \quad (4)$$

$$f_{N-2p}(s) = \Theta(s) \frac{e^{\alpha s^2}}{Z_N} \sum_{k=0}^p (N-2k-s)^{N-1} g_k(s), \quad (5)$$

$$g_0(s) = \frac{(N-1)a(s)}{2^{N-3}s(N+2)!}, \quad (6)$$

$$a(s) = N(s+1)^3 - N^2(s+1) + N + s^3 - 2s, \quad (7)$$

$$g_k(s) = \frac{(-1)^k b_{N-2k}(s)}{s^{2N-3}N(N+2)!} \binom{N}{k}, \quad k \neq 0, \quad (8)$$

$$b_m(s) = s^2N(N-1)[3m+s(N+1)] \\ + [s(N-1)+m] \times \\ \times [6m^2 - N(N+1)(N+2)]. \quad (9)$$

To obtain the long-time asymptotic behavior for $|\alpha| \ll 1$, we integrate Eq. (4) by parts $N-1$ times. We find

$$\delta\mathcal{C}_{11}(t) \underset{t^* \gg 1}{\sim} \sum_{p=0}^{E(N/2)} h_p \cos[(N-2p)(t^* - \pi/2)] \times \\ \times (t^*)^{-N} e^{(N-2p)^2\alpha}/Z_N, \quad (10)$$

$$h_p = \frac{[(N-2p)^2 - N]}{2^{N-3}N} \binom{N}{p} \times \\ \times [1 + (p-1)\delta_{p,N/2}]. \quad (11)$$

For $N = M^2$, one of the terms in Eq. (10) vanishes, as for the four-spin ring. [6] More important, the leading long-time behavior $\propto 1/t^{*N}$, which falls off very rapidly for large N . Although Eq. (10) fails for $|\alpha| \gg 1$, its behavior for $\alpha \neq 0$ is useful to illuminate the dramatic difference between the long-time asymptotic behavior for the FM and AFM cases. For the FM case, $\alpha > 0$, the dominant behavior $\propto \cos[N(t^* - \pi/2)]$, as all of the spins oscillate together. In the AFM case, $\alpha < 0$, the dominant long-time asymptotic behavior is given by the smallest possible oscillation frequency. As shown in the following, $\mathcal{C}_{11}(t)$ is always finite as $T \rightarrow 0$.

As $T, N \rightarrow \infty$, Liu and Müller obtained an analytic form for \mathcal{C}_{11} , but their procedure was not extendable to finite N . [9] From the integral representation, $\mathcal{D}_N(x) = \int_0^\infty 2p^{1-N} \sin^N p \sin(px) dp/\pi$, we expand $\sin^N p/p^N$ as $\exp[-N(p^2/6 + p^4/180 + p^6/2835 + \dots)]$ to obtain a $1/N$ asymptotic expansion for $\mathcal{C}_{11}(t)$ as $T \rightarrow \infty$,

$$\lim_{\substack{T \rightarrow \infty \\ N \gg 1}} \mathcal{C}_{11}(t) \sim [1 + 2e^{-\tilde{t}^2} (1 - 2\tilde{t}^2)]/3 \\ + 2[1 - e^{-\tilde{t}^2} (1 + \tilde{t}^2 - \tilde{t}^4/3 - 2\tilde{t}^6)]/(5N) \\ + \frac{12}{175N^2} \left[1 - e^{-\tilde{t}^2} \left(1 + \tilde{t}^2 - \frac{157}{36}\tilde{t}^4 + \right. \right. \\ \left. \left. \frac{50}{27}\tilde{t}^6 - \frac{97}{108}\tilde{t}^8 + \frac{7}{18}\tilde{t}^{10} \right) \right], \quad (12)$$

where $\tilde{t} = Jt[(N-1)/6]^{1/2}$. From Eq. (12), $\mathcal{C}_{11}(0) = 1$ through order $1/N^2$, as required, and $\mathcal{C}_{11}(t)$ has the correct $N \rightarrow \infty$ limit. [9] However, Eq. (12) is highly accurate for intermediate N values as well. In Fig. 1, we have plotted $\lim_{T \rightarrow \infty} \mathcal{C}_{11}(t)$ for $N = 5, 6, 7, 8, 9, 25, 50, 100, \infty$ as a function of $Jt[(N-1)/6]^{1/2}$. The curves for $N = 25, 50, 100, \infty$ were obtained from Eq. (12), whereas the other curves were generated from the exact solution, Eqs. (4)-(9). Equation (12) is very accurate at short and long times, even for $N = 5$. We note that for $\tilde{t} \lesssim 1$, $\lim_{T \rightarrow \infty} \mathcal{C}_{11}(t)$ is a universal function of $Jt\sqrt{N-1}$, as suggested by the $1/N$ expansion. Although the $N \rightarrow \infty$ curve is exact, and the curves for $N = 50, 100$ are quite accurate, the curve for $N = 25$ exhibits a small ($\approx 1\%$) inaccuracy for $1.2 \lesssim \tilde{t} \lesssim 2.2$.

At arbitrary N, t and $N \gg 1, t \rightarrow \infty$, respectively,

$$\lim_{T \rightarrow \infty} \mathcal{C}_{11}(t) = 1/N + (N-1)[\delta_N + f_N(t)], \quad (13)$$

$$\lim_{t, T \rightarrow \infty} \mathcal{C}_{11}(t) \underset{N \gg 1}{\sim} \frac{1}{3} + \frac{2}{5N} + \frac{12}{175N^2}, \quad (14)$$

$$\delta_N \underset{N \gg 1}{\sim} \frac{175N^2 - 315N + 36}{525N^2(N-1)}. \quad (15)$$

In the inset of Fig. 1, we have compared the exact values of δ_N with those obtained from Eq. (15) for $3 \leq N \leq 65$. For $N = 3$, the differences are noticeable on this curve. As N increases from 5 to 65, the relative difference decreases rapidly from 0.14% to 0.2 ppm. Since the exact formula for δ_N with N odd (even) contains non-trivial contributions of logarithms of all prime numbers from 3 to N (2 to $N/2$), respectively, the extremely good numerical agreement between the exact δ_N and Eq. (15) is remarkable.

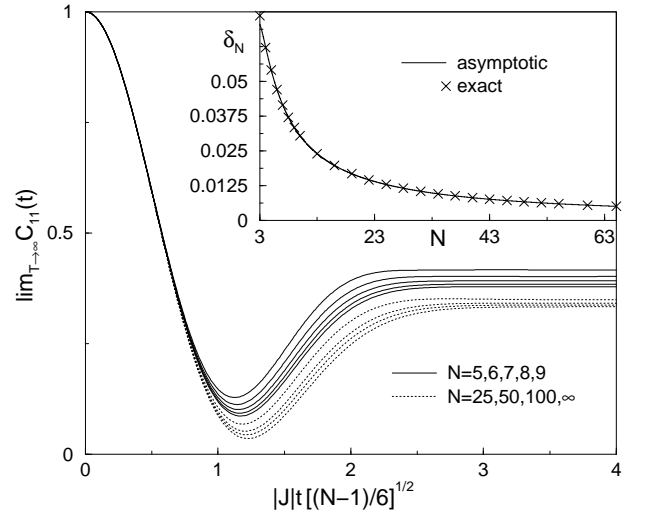


FIG. 1: Plots of $\lim_{T \rightarrow \infty} \mathcal{C}_{11}(t)$ versus $|Jt[(N-1)/6]^{1/2}$, for $N = 5, 6, 7, 8, 9$ from Eqs. (4)-(9) (solid), and for $N = 25, 50, 100, \infty$ from Eq. (12) (dashed). Inset: Plot of the exact (\times) and asymptotic values, Eq. (15), of δ_N .

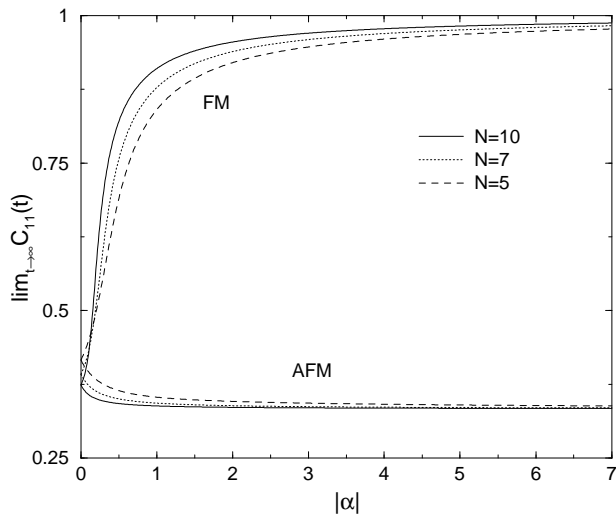


FIG. 2: Plots of $\lim_{t \rightarrow \infty} C_{11}(t)$ versus $|\alpha|$ for $N = 5, 7, 10$ and for both ferromagnetic and antiferromagnetic couplings.

In Fig. 2, we plot the long-time asymptotic limits $\lim_{t \rightarrow \infty} C_{11}(t)$ for both the FM and AFM cases, for $N = 5, 7, 10$, as functions of $|\alpha|$. The FM values approach 1 as $T \rightarrow 0$. But, the low- T AFM values rapidly approach their $T = 0$ asymptotic limit, $\frac{1}{3}$. This indicates the spins are strongly frustrated, since one might naively expect the AFM $\lim_{t \rightarrow \infty} C_{11}(t) = 0$, as for the four-spin ring. [6] In that case, the unfrustrated alternating spin direction configuration was possible. In this AFM case, however, the $N \geq 3$ spins are as frustrated as $T \rightarrow 0$ as are an infinite number of them as $T \rightarrow \infty$.

We now examine the low- T AFM dynamics. In this case, the dominant contributions to the numerator of C_{11} and to Z_N arise from $s \ll 1$. The leading contributions to these integrals are $P_N s^2 e^{-|\alpha|s^2}$ and $Q_N s^2 e^{-|\alpha|s^2}$, respectively, where P_N and Q_N are complicated functions of N , but for arbitrary $N \geq 3$, $P_N/Q_N = \frac{2}{3}$. Thus, as $T \rightarrow 0$, the Fourier transform $\delta C_{11}(\omega)$ of $\delta C_{11}(t)$ attains the exact uniform asymptotic form,

$$|\alpha|^{-1/2} \delta C_{11}(\omega) \underset{T \rightarrow 0}{\sim} \frac{8}{3\sqrt{\pi}} \tilde{\omega}^2 e^{-\tilde{\omega}^2}, \quad (16)$$

where $\tilde{\omega} = |\alpha|^{-1/2} \omega / |J|$. For $N \geq 5$, corrections to Eq. (16) are of $\mathcal{O}(|\alpha|^{-1})$, whereas for $N = 4$, they are of $\mathcal{O}(|\alpha|^{-1/2})$. In Fig. 3, we show the frequency dependence of the low- T AFM mode. Since $C_{11}(t)$ for fixed N is a uniform function of $|J|t/|\alpha|^{1/2}$, the amplitude of $\delta C_{11}(\omega)$ must also be scaled by $|\alpha|^{-1/2}$ for the curves to nearly coincide. Here we plot the curves at $\alpha = -5, -10$ for $N = 4, 7, 10$, obtained from our exact solution, Eqs. (4) - (9). The exact asymptotic form, Eq. (16) is also plotted for comparison. The $N = 4$ curves nearly coincide with the others, but do show some small dependence upon T . However, the $N = 7$ and 10 curves are nearly identical and independent of T , and are nearly indistinguishable

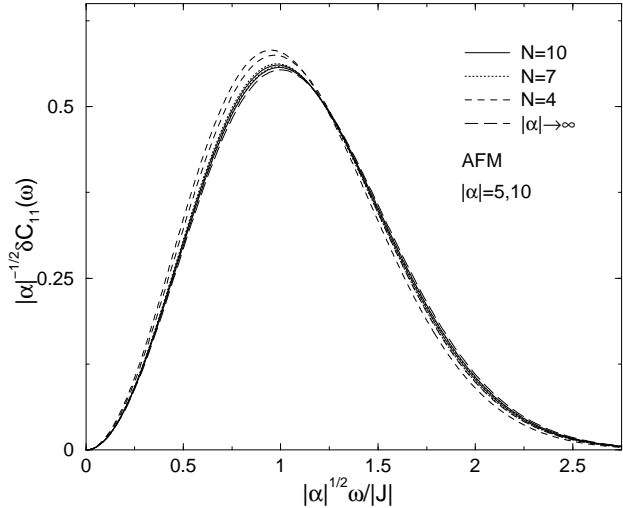


FIG. 3: Plots of the low- T $|\alpha|^{-1/2} \delta C_{11}(\omega)$ versus $|\alpha|^{1/2} \omega / |J|$ for the antiferromagnetic cases with $N = 4, 7, 10$ at $\alpha = -5, -10$. Also shown is the exact $T \rightarrow 0$ limit, Eq. (16).

from the asymptotic curve for $|\alpha| = 10$, when scaled in this manner.

Inverting the Fourier transform, the low- T AFM $C_{11}(t)$ asymptotically approaches

$$C_{11}(t) \underset{T \rightarrow 0}{\sim} [1 + 2e^{-\bar{t}^2} (1 - 2\bar{t}^2)]/3, \quad (17)$$

where $\bar{t} = t^*/(2|\alpha|^{1/2})$. Hence the AFM $\lim_{T \rightarrow 0} C_{11}(t)$ is a uniform function of $(JT)^{1/2}t$, independent of N . Moreover, it has precisely the same form as does $\lim_{N, T \rightarrow \infty} C_{11}(t)$, Eq. (12), pictured in Fig. 1, except for the different scaling factor.

We now turn to the FM case as $T \rightarrow 0$. From Eq. (10), we expect that all of the spins will be oscillating together with frequency NJ . But, this is strictly true only in the $T \rightarrow 0$ limit. At finite α , the oscillation frequency deviates from this value slightly. To determine more precisely the actual nature of the mode, we note that for $\alpha > 1$, the peaks in the integrand and in Z_N both occur within $N - 2 \leq s \leq N$. As $T \rightarrow 0$, we evaluate Z_N by integration by parts, leading to the exact low- T limit of the FM Fourier transform,

$$\delta C_{11}(\omega) \underset{T \rightarrow 0}{\sim} A_N f_N(\omega^*) / f_N(\omega_N^*), \quad (18)$$

where $A_N = 2e[(N-1)/e]^N / N!$, $\omega^* = \omega/J$, and ω_N^* , the position of the exact maximum in $f_N(\omega^*)$, is an eigenvalue of $2\alpha s - (N-2)/(N-s) + d \ln[g_0(s)]/ds = 0$. f_N and g_0 are given by Eqs. (5) and (6), respectively. Approximately, $\omega_N^* \approx N - (N-1)/(2N\alpha)$, and $f_N(\omega^*)$ has a width characterized by a normal Gaussian distribution parameter $\sigma_N = \sqrt{N-1}/(2N\alpha)$. Thus,

$$\delta C_{11}(\omega) \underset{\alpha \gg 1}{\approx} A_N \exp[-(\omega^* - \omega_N^*)^2 / (2\sigma_N^2)]. \quad (19)$$

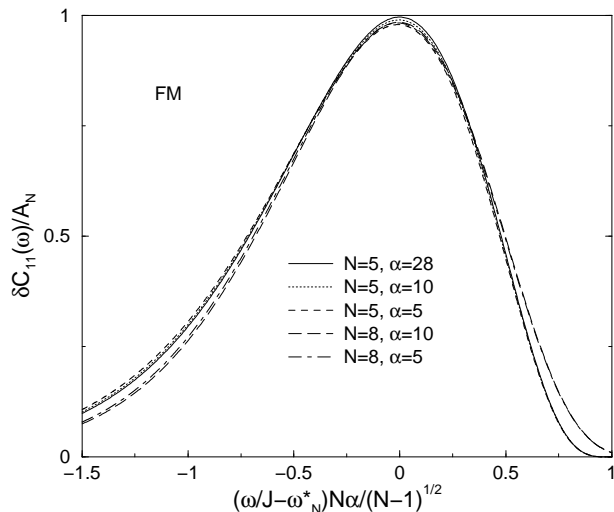


FIG. 4: Plots of the low- T $\delta\mathcal{C}_{11}(\omega)/A_N$ versus $(\omega/J - \omega_N^*)N\alpha/\sqrt{N-1}$, where $\omega_N^* = N - (N-1)/(2N\alpha)$ and $A_N = 2e[(N-1)/e]^N/N!$, for the FM cases with $N = 8$, $\alpha = 5, 10$, and $N = 5$, $\alpha = 5, 10, 28$.

In this Gaussian approximation, ω_N^* , σ_N , and A_N are correctly given to their respective leading orders in $1/\alpha$, but the skewness of the peak is not accurately represented. In Fig. 4, we have therefore plotted the scaled low- T $\delta\mathcal{C}_{11}(\omega)/A_N$ versus $(\omega^* - \omega_N^*)N\alpha/\sqrt{N-1}$, for $N = 8$ at $\alpha = 5, 10$, and for $N = 5$ at $\alpha = 5, 10, 28$, using our exact formulas, Eqs. (4) - (9). The $N = 5$ curves nearly coincide, as do the $N = 8$ curves, and the scaled height approaches 1 as $T \rightarrow 0$. As mentioned previously, the asymmetry of the curves decreases with increasing N , a feature not incorporated in the Gaussian approximation. Nevertheless this scaling procedure works remarkably well, and $N = 5$ is close to the large N limit, even for the FM case.

Inverting the low- T FM Fourier transform, Eq. (19),

$$\mathcal{C}_{11}(t) \underset{T \rightarrow 0}{\approx} 1 - \frac{B_N}{\alpha} \left[1 - e^{-t^2 \sigma_N^2 / 2} \cos(\omega_N^* t) \right], \quad (20)$$

where $B_N = A_N \sqrt{\pi(N-1)}/2N$. As $N \rightarrow \infty$, $B_N \rightarrow 1/N$. The deviation of the long-time limit of Eq. (20) agrees to within 1% with our results presented in Fig. 2. The decay in time of the mode in this approximation is Gaussian, with a lifetime $\tau_N = 1/\sigma_N$. Thus, as $T \rightarrow 0$, the oscillations are characterized by a frequency that approaches NJ linearly in T , a lifetime that diverges as $1/T$, and an amplitude that vanishes as T .

Finally, we remark that our exact results for $\lim_{T \rightarrow \infty} \mathcal{C}_{11}(t)$ in the N -spin equivalent neighbor model may also lead to the correct $T \rightarrow \infty$ limit of the near-neighbor correlation function $\mathcal{C}_{12}(t)$ of N -spin rings with classical Heisenberg near-neighbor exchange coupling.

From Eq. (13) and the sum rule, we conjecture that, as for the N -spin equivalent neighbor model,

$$\lim_{T \rightarrow \infty} \mathcal{C}_{12}(t) = 1/N - \delta_N - f_N(t) \quad (21)$$

for the N -spin ring. In support of this conjecture, we have studied the N -spin systems consisting of M spins \mathbf{s}'_j coupled to $N - M$ spins \mathbf{s}_i on a ring. Letting $\mathbf{s} = \sum_{i=1}^{N-M} \mathbf{s}_i$ and $\mathbf{s}' = \sum_{j=1}^M \mathbf{s}'_j$, the Hamiltonian is

$$H = -J \sum_{i=1}^{N-M} \mathbf{s}_i \cdot \mathbf{s}_{i+1} - J' \mathbf{s} \cdot \mathbf{s}', \quad (22)$$

where $\mathbf{s}_{N-M+1} = \mathbf{s}_1$, which is integrable. [10] Setting $\mathcal{C}'(t) = \langle \mathbf{s}'(t) \cdot \mathbf{s}'(0) \rangle$, we found for $N - M = 3$, $M = 1, 2, 3$, and for $N - M = 4$, $M = 1, 2$, that

$$\lim_{T \rightarrow \infty} \mathcal{C}'(t) = M^2/N + M(N - M)[\delta_N + f_N(t)]. \quad (23)$$

Most significant of these is the result for the four-spin ring with $M = 2$. We also showed previously that Eq. (21) is valid for four- and three-spin rings. [6, 7]

In summary, we have solved exactly for the time auto-correlation function $\mathcal{C}_{11}(t)$ of a spin in the N -spin equivalent neighbor model. As $T \rightarrow \infty$, $\mathcal{C}_{11}(t) \propto t^{-N}$ for $Jt \gg 1$, curves for different N exhibit very similar shapes when plotted as functions of $|J|t[(N-1)]^{1/2}$, and an accurate $1/N$ asymptotic expansion is found. At low T , the antiferromagnetic $\mathcal{C}_{11}(t)$ is a universal function of $tT^{1/2}$, independent of N , and exhibiting strong frustration. For the ferromagnetic case at low T , there is a single mode with a peak position at $\approx NJ - k_B T(N-1)/N$, and a shape that fits an accurate scaling relation. We conjecture that the $T \rightarrow \infty$ limit of the near-neighbor correlation functions $\mathcal{C}_{12}(t)$ for the N -spin equivalent neighbor model and for the N -spin ring may be identical.

* Electronic address: rklemm@mpipks-dresden.mpg.de

† Electronic address: marco@mpipks-dresden.mpg.de

- [1] D. Gatteschi, A. Caneschi, L. Pardi, and R. Sessoli, *Science* **265**, 1054 (1994).
- [2] A. Lascialfari *et al.*, *Phys. Rev. B* **55**, 14341 (1997).
- [3] M.H. Julien *et al.*, *Phys. Rev. Lett.* **83**, 227 (1999).
- [4] R. Caciuffo *et al.*, *Phys. Rev. Lett.* **81**, 4744 (1998).
- [5] M. Luban and J. Luscombe, *Am. J. Phys.* **67**, 1161 (1999).
- [6] R. Klemm and M. Luban, *Phys. Rev. B* **64**, 104424 (2001), (see also cond-mat/0105050).
- [7] M. Ameduri and R. Klemm, cond-mat/0108213.
- [8] C. Kittel and H. Shore, *Phys. Rev.* **138**, A1165 (1965).
- [9] J.-M. Liu and G. Müller, *Phys. Rev. B* **44**, 12020 (1991).
- [10] N. Srivastava *et al.*, *Z. Phys. B* **70**, 251 (1988).